Available online at www.sciencedirect.com

SciVerse ScienceDirect

Ceramics International 39 (2013) 7649–7655

CERAMICS INTERNATIONAL

www.elsevier.com/locate/ceramint

Experimental investigation of thermo-physical properties of platelet mesoporous SBA-15 silica particles dispersed in ethylene glycol and water mixture

Azadeh Tadjarodi[a,*], Fatemeh Zabihi[a,b], Shahrara Afshar[a]

[a]Department of Chemistry, Iran University of Science and Technology, 16846-13114 Tehran, Iran
[b]Chemistry and Nanotechnology Laboratory, National Center for Laser Science and Technology, Tehran, Iran

Received 1 January 2013; received in revised form 14 February 2013; accepted 25 February 2013
Available online 27 March 2013

Abstract

This paper presents an experimental investigation of thermophysical properties of platelet mesoporous SBA-15 particles dispersed in 60:40 (v/v) ethylene glycol:water mixture. The effect of weight fraction of particles and temperature is studied on density, viscosity and thermal conductivity of nanofluids. The maximum measured thermal conductivity enhancement reaches up to 22% for the nanofluids containing 5 wt% of SBA-15 at 60 °C. The SBA-15 nanofluids show Newtonian behavior in the tested temperature range. Also, the relative density increases between 0.4% and 2.2% when the weight percent of the nanoparticles varies between 1 and 5 at 60 °C. Structural and morphological characterization of synthesized SBA-15 have been carried out using Fourier transform infrared spectroscopy (FTIR), Scanning electron microscopy (SEM), X-ray powder diffraction (XRD) and N_2 adsorption–desorption isotherms methods.

Keywords: B. Porosity; B. Platelets; C. Thermal properties; D. SiO_2

1. Introduction

Today, the conventional heat transfer fluids such as water, ethylene glycol and engine oil have various industrial applications including microelectronics, energy supply, transportation, heating, ventilating and air-conditions [1]. However, the limitation in thermal properties of these fluids such as poor thermal conductivity has led researchers to find ways for enhancing the thermal transport properties to improve the energy efficiency of the system. It is well known that the metals and metal oxides have much higher thermal conductivity than the conventional heat transfer fluids [2]. Therefore, since Maxwell's theoretical work was published more than 100 years ago, the researchers have tried to increase the thermal conductivity of the base fluids by suspending micro or larger sized solid particles in the fluids [3]. But using suspensions containing micro or millimeter-sized particles will be exposed to many difficulties, such as sedimentation of particles, corrosion of equipment and higher pumping power requirement [4]. In the last two decades, the fascinating advances in nanotechnology have introduced a new kind of heat transfer fluid, called as nanofluid. Nanofluids are colloidal mixture of nanoparticles and a base liquid [5]. The surface/volume ratio of nanoparticles is 1000 times larger than that of microparticles. The use of nanometer-sized particles with a large specific area could improve the heat transfer. Also according to higher stabilization, the Stokes theory provides against the particle sedimentation and prevents clogging of the heat sink [6]. So, due to their superior enhanced thermal properties, nanofluids have attracted great interests recently. The thermal properties, including: thermal conductivity, viscosity, specific heat, convective heat transfer coefficient and critical heat flux have been studied extensively [7]. Among all, the thermal conductivity is the first referred one, and it is believed to be the most important parameter responsible for the enhanced heat transfer. Experimental studies on the thermal conductivity of nanofluids containing Al_2O_3, TiO_2, SiO_2, CuO, Cu, Ag, Au, Pd, etc. nanoparticles, have been reported by many researchers [8–12]. Among these, because of the high thermal and chemical

*Corresponding author. Tel.: +98 21 7724 0516; fax: +98 21 7749 1204.
E-mail address: tajarodi@iust.ac.ir (A. Tadjarodi).

0272-8842/$ - see front matter © 2013 Elsevier Ltd and Techna Group S.r.l. All rights reserved.
http://dx.doi.org/10.1016/j.ceramint.2013.02.103

stability and the electrical insulation, silica containing nanofluids can be very important to certain industries for example in high voltage applications where cooling is required. [13]. Although some experimental and theoretical works focused on the silica nanofluids [14–25], there have been very few reports on the study of mesoporous silica ($mSiO_2$) nanofluid for enhancement heat transfer properties [26,27]. Mesoporous silica particles, which was first produced by Mobil Corporation Laboratories in 1992, has received great attention because of its uniform pores with high specific surface area in applications such as medicine, biosensors, imaging and catalysis [28]. Since heat transfer is a surface phenomenon at the particle–fluid interface, its magnitude will increase with an increase in the surface area of the particles. Therefore, enhancement in thermal conductivity in nanofluids containing porous nanoparticles is expected due to the enhancement of the surface area of the nanoparticles. Amrollahi et al. [26] studied the water based $mSiO_2$ nanofluid. They dispersed $mSiO_2$ nanoparticles in water using ultrasonic probe and showed that spending 24 h for preparation of a nanofluid containing 2.5 v% of nanoparticles resulted in a 7% increase in the thermal conductivity of the based fluid. Nikkam et al. [27] prepared aqueous dispersion of mesoporous silica in the range of 1–6 wt% by adjusting the pH of the nanofluids using an ultrasonic device. Measurement of the thermal conductivity of nanofluids at different temperatures showed that the maximum thermal conductivity enhancement of ~4.1% was obtained for 6 wt% at 60 °C.

The effectiveness of the nanofluids coolants depends on the flow mode (laminar or turbulent) and can be estimated based on the fluid dynamic equations. Viscosity and density are important properties to determine nanofluids dynamic and heat transfer properties [29]. Limited investigations are reported on the viscosity of dense and mesoporous silica nanofluids [13,27,30]. All the reported results show that the viscosity of nanofluids increases with the increase in the concentration of the nanoparticles, and decreases with an increase in the temperature. Also, Numburu et al. [31] studied the effect of silica nanoparticles diameter on the viscosity of SiO_2 nanofluids. They showed that the viscosity of nanofluids decreases with increasing in the nanoparticles diameter.

In this work, we synthesized mesoporous SBA-15 nanoparticles with platelet morphology. Also the effects of weight fraction of synthesized nanoparticles have been investigated on thermo-physical properties of ethylene glycol–water based nanofluids at various temperatures. To our knowledge, this is the first report on thermo-physical properties of ethylene glycol–water (EG/W 60:40 v/v) based suspension containing mesoporous silica nanoparticles. Among the various heat transfer fluids, in cold climates, ethylene glycol or propylene glycol mixed with water in different volume percentages are typically used as a heat transfer fluid for automobiles, heat exchangers and industrial coolants [32]. Ethylene glycol or propylene glycol lowered the freezing point of water and its volatility. These fluids do not freeze even if the operating temperature reaches down to –40 °C. Under low temperature, ethylene glycol/water mixture has better properties than propylene glycol/water mixture. The questions arise as whether our proposed methods are general and whether it is possible to develop modified mesoporous silica with better properties and performance?

2. Experimental

2.1. Materials and reagents

All materials were of analytical reagent grade. P123 (poly (ethylene oxide)–poly(propylene oxide)–poly(ethylene oxide) (EO_{20}–PO_{70}–EO_{20})) was obtained from Sigma-Aldrich Chemical Co. Tetraethylorthosilicate (TEOS 98%), hydrochloric acid (HCl 37%), zirconium (IV) oxide chloride octahydrate ($ZrOCl_2 \cdot 8H_2O$) were obtained from Merck Chemical Co.

2.2. Synthesis of platelet mesoporous silica (SBA-15)

Synthesis of platelet SBA-15 is done according to the literature [33] with slight modification. In a typical experiment, 0.32 g of $ZrOCl_2 \cdot 8H_2O$ was dissolved in 80 mL of HCl (2 M) solution at 40 °C. After the solution turned clear, 2 g of P-123 was added to the acidic solution and stirred (450 rpm) for about 2 h. Then, 4.5 mL TEOS was injected to the above solution at the injection rate of 30 mL h^{-1}. The mixture was sealed in a polypropylene bottle, stirred at 40 °C for 24 h, and then hydrothermally heated at 100 °C under static conditions for another 24 h. The solid product was washed with water and dried at room temperature. Extraction of P123 template was performed by calcinations at 600 °C for 6 h (heating rates of 1 °C/min) in air.

2.3. Preparation of nanofluids

Nanofluids with particle weight of 1%, 3% and 5% were prepared by dispersing the specific amount of SBA-15 nanoparticles in EG/W mixture using a magnetic stirrer for about 6 h and then ultrasonicating the suspension for 2 h using a 280 W ultrasonicator. This device is used to break large agglomerates of nanoparticles in the fluid and make stable suspension. No surfactant was used as they may have some influence on the thermo-physical properties of nanofluid. It was observed with naked eyes that the nanofluids were uniformly dispersed for 48 h.

2.4. Characterization of synthesized nanoparticles and measurement of thermophysical properties

Characterization of the samples is performed by different conventional techniques. X-ray powder diffraction (XRD) data are acquired on Philips X-pert diffractometer using CuKα radiation. SEM images are taken by Philips XL-300 instrument. FT-IR spectra were recorded on a NEXUS 670 FT-IR spectrometer. N_2 adsorption–desorption isotherms were measured on a NOVA STATION B instrument at 77 K. Specific surface area was calculated according to the Brunaure–Emmet–Teller (BET) method, and the pore-size distribution was calculated using desorption branch of the isotherm by the

Barrett–Joyner–Halenda (BJH) method. The thermal conductivity of nanofluids was measured by using KD2-Pro thermal properties analyzer (Decagon Devises, USA), which is based on the transient hot wire method. The probe sensors used for these measurements are of length 60 mm and of diameter 1.3 mm (KS-1). The viscosity of nanofluids was measured by a Brookfield Viscometer (LV DV-II+ Pro EXTRA, USA) with a small sample adapter. The adapter consists of a cylindrical sample holder, a water jacket and a spindle which is immersed in the test fluid. The viscometer can provide a rotational speed that can be controlled to vary from 0.01 to 200 rpm yielding the shear rate from 0.01 to 264 s^{-1}. It measures viscosity by measuring the viscous drag of the fluid against the spindle when it rotates. The spindle type and speed combinations will produce satisfactory results when the applied torque is between 10% and 100%. In order to study the temperature effect, a thermostat bath was used to ensure all the measurements are at constant temperature. The density of nanofluids was measured by a digital density meter (KEM, DA 650, Japan). The fluid sample is injected into an oscillating U-shaped tube, which has an electronic system for excitation, frequency counting and display. To carry out accurate measurements, an observation window is provided to check whether the tube is completely filled with the sample without any air bubbles in it.

3. Results and discussion

3.1. Characterization of the samples

The small and wide angle XRD patterns of SBA-15 are depicted in Fig. 1. The three distinct Bragg diffractions in the small angle XRD patterns, (100), (110), and (200), are characteristic of a highly ordered two-dimensional hexagonal mesoscopic structure having space group symmetry P6mm of pure SBA-15 [34]. The inset of Fig. 1 shows wide angle XRD patterns. The pattern showed a broad peak at 2θ value of 20–30° indicating the amorphous nature of the silica particles.

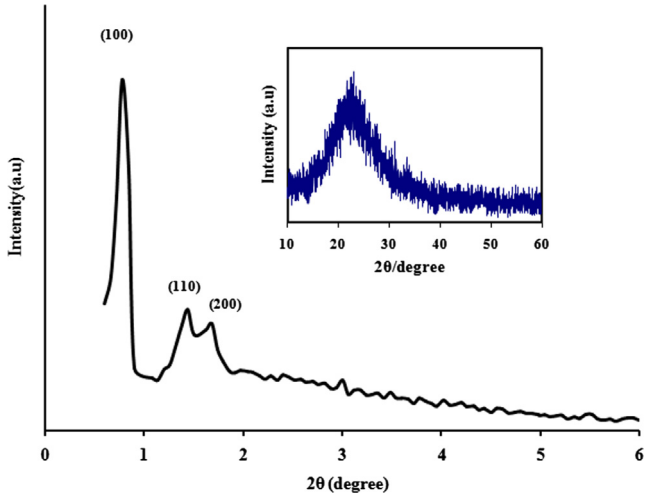

Fig. 1. Low angle XRD pattern of mesoporous silica SBA-15. The inset shows wide angle XRD pattern of particles.

FT-IR spectra of SBA-15 are shown in Fig. 2. SBA-15 gives a broad band around 3000–3600 cm^{-1} and the sharp band at 1604 cm^{-1} which can be assigned to the symmetrical stretching vibration modes of O–H and deformation of the adsorbed water molecules, respectively. Absorption bands at 470, 856 and 1110 cm^{-1} are related to the bending, symmetric and asymmetric stretching vibrations of Si–O–Si bonds, respectively [35].

The formation of SBA-15 with platelet morphology was confirmed by SEM images (Fig. 3). The SEM images reveal the hexagonal disk-shape morphology. The channel directions of the 2D-hexagonal structures were parallel to the thickness direction of the hexagonal platelet morphology. The average width and thickness of the platelets are 600–800 nm and 200–250 nm, respectively using the Microstructure Measurement program.

Fig. 4 shows N_2 adsorption–desorption isotherms. SBA-15 with obtained specific surface area equal to 690.1 m^2/g and average pore size of 9.76 nm shows a type IV isotherm with sharp capillary condensation step at relative pressures (P/P_0) of 0.76–0.84, with an H1 type hysteresis loop. It is interesting to notice that desorption branch of this material did not follow the same trend as adsorption branch in H1 hysteresis. The wall thickness for SBA-15 (4.34 nm) was calculated using the following equation [36]:

$$\text{Wall thickness} = \frac{2d_{100}}{\sqrt{3}} - \text{BJH average pore diameter}$$

Table 1 has been listed the pore structure parameters of SBA-15.

3.2. Thermo-physical properties

3.2.1. Viscosity of nanofluids

In order to verify the accuracy of the experimental data, initial measurements are done with the known viscosity of the base fluid (60:40% EG/W) at temperature range from 10 to 60 °C and the obtained values are compared with the reported values [37]. As shown in Fig. 5, it is apparently seen that the measured viscosity data have an excellent agreement with the given data in ASHRAE handbook [37]. So, the instrument can be comfortably used to measure the viscosity of the nanofluids.

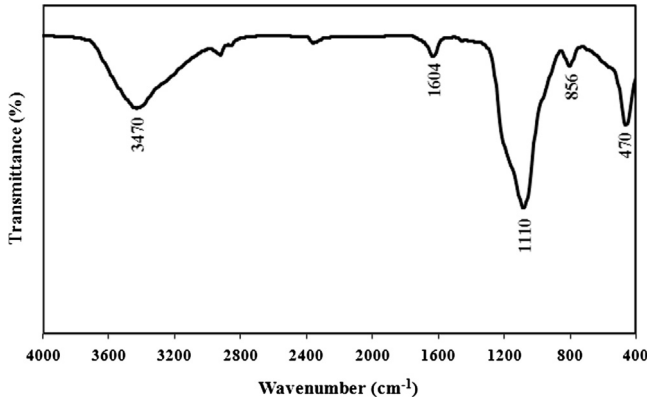

Fig. 2. FTIR spectra of mesoporous silica SBA-15.

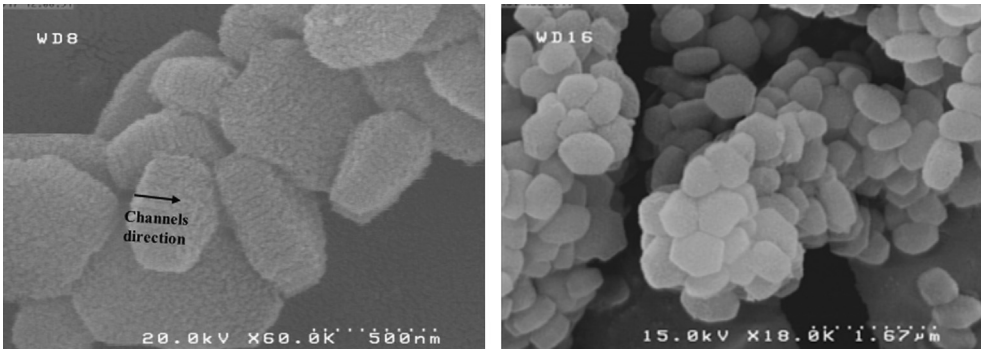

Fig. 3. SEM image of the platelet mesoporous silica SBA-15.

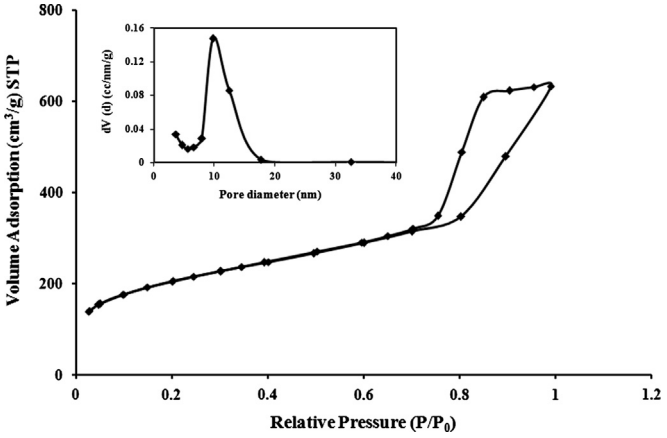

Fig. 4. N_2 adsorption–desorption isotherms of SBA-15. The inset shows the BJH pore-size distribution calculated from the desorption branch of the isotherm.

Table 1
The structural parameters of the SBA-15 particles.

Sample ID	BET surface area (m^2/g)	Pore size (nm)	Pore volume (cm^3/g)	d_{100} (nm)
SBA-15	690.1	9.76	1.176	11.3

The next step was to determine whether the base fluid and nanofluids are obeying the Newtonian behavior or not. For a non-Newtonian fluid, the viscosity depends on the shear rate. The equation governing Newtonian behavior of a fluid is given by $\tau = \mu\gamma$, where τ is the shear stress, μ is the coefficient of viscosity and γ is the shear strain rate. The initial experiments were carried out for the EG/W mixture. The results show that the measured shear stress depends linearly on the shear rate. These results match well with the reported values [37]. Also, after the addition of SBA-15 nanoparticles, it is observed that shear stress for all the concentrations of nanofluids increases linearly with increasing the shear rate. Since EG/W mixture exhibits Newtonian behavior, it dominates the whole nanofluids behave like a Newtonian fluid at measured concentrations of nanoparticles. The shear stress versus shear rate for 5 wt% SBA-15 nanofluids at different temperatures is shown in Fig. 6. Irrespective of small intercept on the shear stress axis due to the uncertainty in the measurements, SBA-15 nanofluid

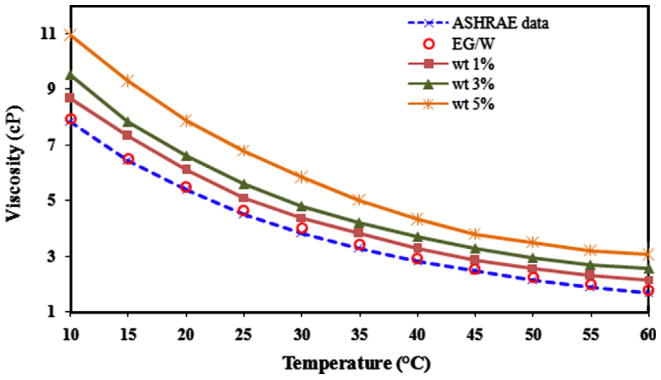

Fig. 5. Viscosity of base fluid and nanofluids as a function of temperature.

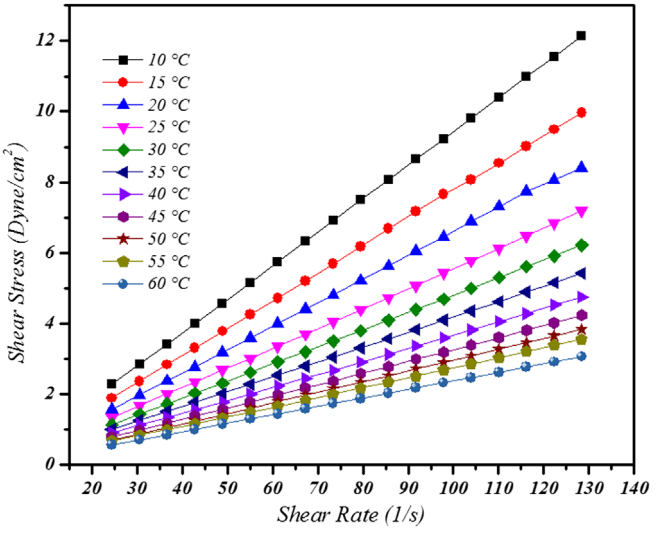

Fig. 6. Shear stress versus shear rate for wt 5% SBA-15 nanofluid at different temperatures.

clearly shows Newtonian behavior. On the other hand, it is observed that the inclination of lines decreases with an increase of temperature from 10 to 60 °C. In the case of Newtonian fluids the slope represents the viscosity of nanofluids. Therefore, we can conclude that the viscosity decreases with an increase in temperature. A similar trend was also observed for nanofluids with 1% and 3% concentrations of SBA-15 nanoparticles.

After performing the initial experiments, viscosity measurements of nanofluids with different concentration of SBA-15 nanoparticles were carried out at various temperatures. It can be seen from Fig. 5, that at any concentration, the viscosity of nanofluid decreases with increasing temperature, which can be attributed to the decrease in inter-particle and inter-molecular adhesive forces [38]. In this case, this behavior could be due to the hydrogen bonding strength deduction between the nanoparticles together and base fluid molecules while the temperature increases. Also, the viscosity of nanofluids increases with increasing the nanoparticles concentrations. The viscosity values at 10 °C of the base fluid is equal to 7.92 cP, while for 1, 3 and 5 wt% SBA-15 nanofluids the viscosity values are 8.66, 9.51 and 10.94 cP, respectively. With an increase in the nanoparticle concentration, the more number of the nanoparticles come into contact with the base fluid. Therefore, the total surface area in contact with the base fluid as well as resistance to the movement of the base fluid molecules increases. Consequently, the viscosity of the nanofluids increases.

Fig. 7 illustrates the relative viscosity ratio of nanofluids with respect to the weight percent of the SBA-15 at various temperatures. The relative viscosity ratio defined as $\mu_r=(\mu_{nf}/\mu_f)$, which subscript *nf* and *f* represent nanofluids and fluid, respectively. As shown in Fig. 7 the relative viscosity increments as temperature increases at a higher rate for higher concentrations of nanoparticles. At 60 °C, the viscosity of 1%, 3% and 5% wt fractions are 1.21, 1.42 and 1.70 times more compared to the base fluid, respectively. Whereas these values, at 10 °C, come to be 1.10, 1.20 and 1.38 times. However, it is noticed that the increment in relative viscosity respect to temperature is not very impressive and representing the high efficiency of our nanofluids. Low relative viscosity for SBA-15 nanofluid at the tested temperature range makes it suitable for cooling applications with minimum pumping power. The maximum relative viscosity for 5 wt% at 60 °C is below 1.7 cp. This value is lower than the results reported in the previous literature for EG/W (60:40) nanofluids. Sundar et al. [39] showed the maximum relative viscosity of the Fe_3O_4 nanofluids at 1% volume fraction at 50 °C is about 3 cp. According to Kumaresan and Velraj [40] research, the MWCNT nanofluids at 0.15% volume fraction show 3.2 times enhancements in viscosity at 40 °C.

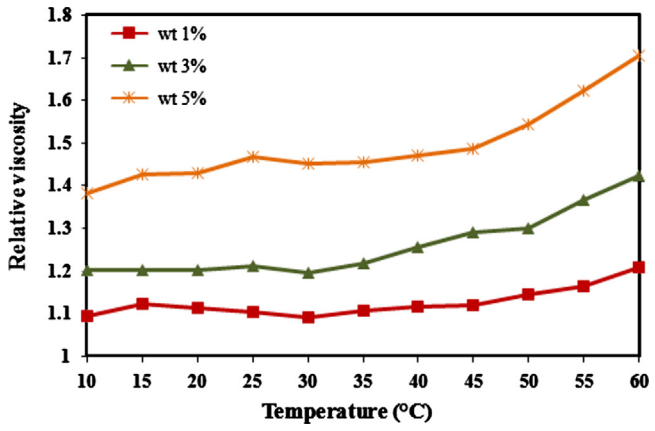

Fig. 7. Relative viscosity of nanofluids at different temperatures.

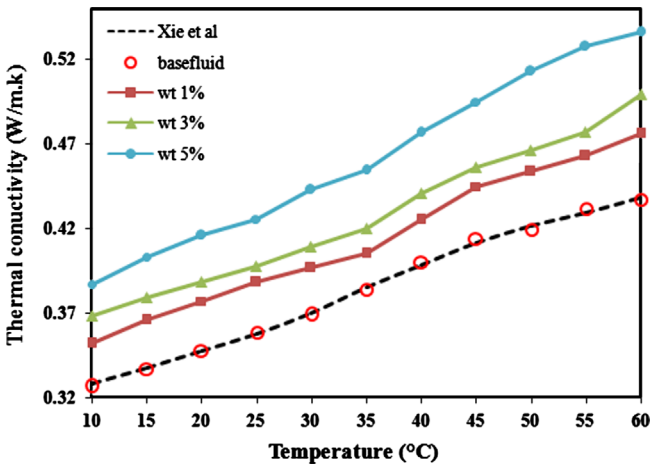

Fig. 8. The temperature dependence of nanofluids thermal conductivity.

3.2.2. Thermal conductivity of nanofluids

To verify the accuracy of our equipment and experimental procedure, initially the thermal conductivity of the base fluid (60:40% EG:W) at different temperatures were measured. Recently, Xie et al. [41] developed an empirical equation that shows the relation between the thermal conductivity of a two fluid mixture and the volume fraction of these two fluids.

$$K_m = \varnothing_w K_w + \varnothing_e K_e - 0.1715\varnothing_w\varnothing_e$$

where, K is the thermal conductivity, $\varnothing$ is the volume fraction, subscripts m, w and e represent fluid–fluid mixture, water and ethylene glycol, respectively. As shown in Fig. 8, our experimental results match well with the above equation values. Following this verification, thermal conductivity measurements of the nanofluids with different concentration of SBA-15 nanoparticles were carried out at various temperatures. The results show that the thermal conductivities of SBA-15 nanofluids increases with increasing the temperature as well as with the weight fraction of nanoparticles. The effect of increasing weight fraction on thermal conductivity enhancement is due to the conversion of suspension to the gel like form and decreasing the particle–particle distances. Thus the nanoparticles form long chain of interconnected networks, which acted as conducting path. This is due to the percolation effect. Based on this effect, the frequency of lattice vibration increases [42]. Similar behavior of silica colloid in concentrated state was observed by Shalkevich et al. [43].

On the other hand, as shown in Fig. 8, the thermal conductivity of the base fluid increases with increasing temperature. This behavior of the base fluid is due to the changes in the hydrogen bonding network with temperature. At low temperatures, instead of energy being transferred between the molecules of fluid, it is stored in hydrogen bonding network. But the increasing of temperature leads to have a high thermal conductivity because of less energy in the hydrogen bonding network [44]. The similar behavior of thermal conductivity of SBA-15 nanofluids with temperature shows that at the tested concentration of nanoparticles, the thermal conductivity of nanofluids is dominated by the thermal conductivity of the base fluid. In addition, increasing the

temperature causes the decreasing of the viscosity of basefluids and more active Brownian motions of the suspended SBA-15 nanoparticles. The Brownian motion induces micro convection causing thermal conductivity enhancement with the increase in temperature [45]. Our results show ~22% enhancement in thermal conductivity for nanofluids containing 5% weight fraction at 60 °C. This value is much higher than the results reported by Nikkam et al. [27]. The main reason for this contrast may be caused by several factors such as difference in the particle size, surface area, nature of the base fluids, method of nanofluid preparation, or even the measurement technique. Timofeeva et al. [46] reported that the addition of nanoparticles in mixture of EG/H_2O based nanofluids results higher enhancements in thermal conductivity than in H_2O at the same particle concentrations and sizes. Yoo et al. [47] investigated the effect of surface area of nanoparticles on the enhancement of the thermal conductivity of the nanofluids. They stated that with increasing the surface area, the interface between the particles and the base fluid increases. Therefore, a dramatic enhancement in thermal conductivity is expected. Because of the lack of any data about the surface area of nanofluids containing mesoporous nanoparticles [26,27], we cannot compare our experimental data with earlier literatures.

3.2.3. *Density of nanofluids*

At first, the density equation of 60:40 EG/W mixture as a function of temperature was obtained in a polynomial form using ASHRAE data [37], then the measured density data of base fluid was compared with this equation, which is given in the following form:

$$\rho_{nf} = -2E{-}0.6T^2{-}0.0004T + 1.0946 \quad \text{with} \quad R^2 = 1$$

As shown in Fig. 9, it is apparently seen that the measured density data of base fluid have an excellent agreement with the handbook data. Following this verification, density measurements of the nanofluids with different concentration of SBA-15 nanoparticles were carried out at various temperatures. The density behavior of the nanofluids is coincident with the base fluid, as ρ decreases with increasing temperature. Also the density of the nanofluids increases with increasing the concentration of nanoparticles. So, relative density percent, $[(\rho_{nf}-\rho_f)/\rho_f] \times 100$, increases between 0.4 and 2.2 were observed when the weight percent of nanoparticles varied between 1 and 5 at 60 °C.

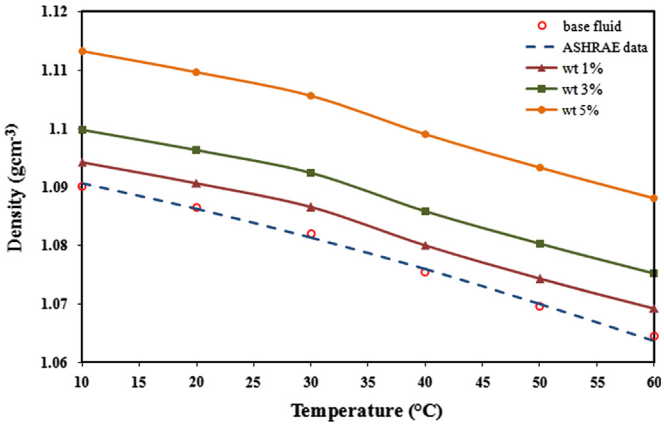

Fig. 9. Density variations of nanofluids with temperatures.

4. Conclusion

In this work, we prepared SBA-15 nanofluids using 60 v% ethylene glycol and 40 v% water mixture as base fluid. The effect of temperature and weight fraction of nanoparticles is experimentally investigated on viscosity, thermal conductivity and density of nanofluids. The maximum relative viscosity for 5 wt% at 60 °C is below 1.7 cp. Low relative viscosity for the nanofluid at the tested temperature range makes it suitable for cooling applications with minimum pumping power. Also, the viscosity of nanofluids decreases with increasing temperature, while the thermal conductivity of the nanofluids increases and reach up to 22% for 5 wt% at 60 °C. These results indicate that the increment of thermal conductivity can be attributed to Brownian motion of suspended SBA-15 nanoparticles as are prone to take place when the viscosity of the base fluid decreases. The micro convection caused by the Brownian motions would have to enhance the thermal conductivity of the suspensions.

References

[1] H. Zhou, C. Zhang, S. Liu, Y. Tang, Y. Yin, Effects of nanoparticles clustering and alignment on thermal conductivities of Fe_3O_4 aqueous nanofluids, Applied Physics Letters 89 (2006) 23123–23125.
[2] S.A. Putnam, D.G. Cahill, P.V. Braun, Z. Ge, R.G. Shimmin, Thermal conductivity of nanoparticle suspensions, Journal of Applied Physics 99 (2006) 84308–84314.
[3] J.C. Maxwell, A Treatise on Electricity and Magnetism, 2nd ed, Oxford University Press, Cambrige, Oxford, 1904, pp. 435–441.
[4] S.K. Das, N. Putra, P. Thiesen, W. Roetzel, Temperature dependence of thermal conductivity enhancement for nanofluids, Journal of Heat Transfer 125 (2003) 567–574.
[5] S. Lee, S.U.S. Choi, S. Li, J.A. Eastman, Measuring thermal conductivity of fluids containing oxide nanoparticles, ASME Journal of Heat Transfer 121 (1999) 280–288.
[6] E.V. Timofeeva, W. Yu, D.M. France, D. Singh, J.L. Routbort, Nanofluids for heat transfer: an engineering approach, Nanoscale Research Letters 6 (2011) 182–188.
[7] X.Q. Wang, A.S. Mujumdar, Heat transfer characteristics of nanofluids: a review, International Journal of Thermal Science 46 (2007) 1–19.
[8] S. Lee, S.U.S. Choi, S. Li, J.A. Eastman, Measuring thermal conductivity of fluids containing oxide nanoparticles, Journal of Heat Transfer 121 (1999) 280–289.
[9] S.M.S. Murshed, K.C. Leong, C. Yang, Enhanced thermal conductivity of TiO_2–water based nanofluids, International Journal of Thermal Sciences 44 (2005) 367–373.
[10] Y. Xuan, Q. Li, Heat transfer enhancement of nanofluids, International Journal of Heat and Fluid Transfer 21 (2000) 58–64.
[11] T.K. Hong, H.S. Yang, C.J. Choi, Study of the enhanced thermal conductivity of Fe nanofluids, Journal of Applied Physics 97 (2005) 1–4.
[12] H.E. Patel, S.K. Das, T. Sundararagan, A.S. Nair, B. Geoge, T. Pradeep, Thermal conductivities of naked and monolayer protected metal nanoparticle based nanofluids: manifestation of anomalous enhancement and chemical effects, Applied Physics Letters 83 (2003) 2931–2933.
[13] R. Kathiravan, R. Kumar, A. Gupta, R. Chandra, Preparation and pool boiling characteristics of silver nanofluids over a flat plate heater, Heat Transfer Engineering 33 (2012) 69–78.

[14] A.K. Nayak, R.K. Singh, P.P. Kulkarni, Measurement of volumetric thermal expansion coefficient of various nanofluids, Technical Physics Letters 36 (2010) 26–31.
[15] D.V. Kuznetsov, S.P. Bardakhanov, A.V. Nomoev, S.A. Novopashin, V.Z. Lygdenov, Heat conductivity of nanofluids based on Al_2O_3, SiO_2, and TiO_2, Journal of Engineering Thermophysics 19 (2010) 138–143.
[16] Y.J. Hwang, Y.C. Ahn, H.S. Shin, C.G. Lee, G.T. Kim, H.S. Park, J.K. Lee, Investigation on characteristics of thermal conductivity enhancement of nanofluids, Current Applied Physics 6 (2006) 1068–1071.
[17] Y. Hwang, J.K. Lee, C.H. Lee, Y.M. Jung, S.I. Cheong, C.G. Lee, B.C. Ku, S.P. Jang, Stability and thermal conductivity characteristics of nanofluids, Thermochimica Acta 455 (2007) 70–74.
[18] X. Yang, Z.H Liu, A kind of nanofluid consisting of surface-functionalized nanoparticles, Nanoscale Research Letters 5 (2010) 1324–1328.
[19] A.N. Turanov, Y.V. Tolmachev, Heat and mass transport in aqueous silica nanofluids, Heat and Mass Transfer 45 (2009) 1583–1588.
[20] S. Ferrouillat, A. Bontemps, J.P. Ribeiro, J.A. Gruss, O. Soriano, Hydraulic and heat transfer study of SiO_2/water nanofluids in horizontal tubes with imposed wall temperature boundary conditions, International Journal of Heat Fluid Flow 32 (2011) 424–439.
[21] C. Wu, T.J. Cho, J. Xu, D. Lee, B. Yang, M.R. Zachariah, Effect of nanoparticle clustering on the effective thermal conductivity of concentrated silica colloids, Physical Review E 81 (2010) 11406–11412.
[22] J.R. Vázquez Peñas, J.M. Ortiz de Zárate, M. Khayet, Measurement of the thermal conductivity of nanofluids by the multicurrent hot-wire method, Journal of Applied Physics 104 (2008) 44314–44322.
[23] M. Jahanshahi, S.F. Hosseinizadeh, M. Alipanah, A. Dehghani, G.R. Vakilinejad, Numerical simulation of free convection based on experimental measured conductivity in a square cavity using water/SiO_2 nanofluid, International Communications in Heat and Mass Transfer 37 (2010) 687–694.
[24] G. Chen, W. Yu, D. Singh, D. Cookson, J. Routbort, Application of SAXS to the study of particle-size-dependent thermal conductivity in silica nanofluids, Journal of Nanoparticle Research 10 (2008) 1109–1114.
[25] D.P. Kulkarni, P.K. Namburu, H.E. Bargar, D.K. Das, Convective heat transfer and fluid dynamic characteristics of SiO_2 ethylene glycol/water nanofluid, Heat Transfer Engineering 29 (2008) 1027–1035.
[26] A. Amrollahi, A.A. Hamidi, A.M. Rashidi, Preparation of MCM-41 nanofluid and an investigation of Brownian movement of the nanoparticles on the nanofluid conductivity, International Journal of NanoScience and Nanotechnology 3 (2007) 13–20.
[27] N. Nikkam, M. Saleemi, M.S. Toprak, S. Li, M. Muhammed, E. B. Haghighi, R. Khodabandeh, B. Palm, Novel nanofluids based on mesoporous silica for enhanced heat transfer, Journal of Nanoparticle Research 13 (2011) 6201–6206.
[28] L.F. Giraldo, B.L. López, L. Pérez, S. Urrego, L. Sierra, M. Mesa, Mesoporous silica applications, Macromolecular Symposia 258 (2007) 129–141.
[29] P.D. Shima, J. Philip, B. Raj, Synthesis of aqueous and nonaqueous iron oxide nanofluids and study of temperature dependence on thermal conductivity and viscosity, Journal of Physical Chemistry C 14 (2010) 18825–18833.
[30] D.P. Kulkarni, P.K. Namburu, H.E. Bargar, D.K. Das, Convective heat transfer and fluid dynamic characterization of SiO2 ethylene glycol/water nanofluids, Heat Transfer Engineering 29 (2008) 1027–1035.
[31] P.K. Namburu, D.P. Kulkarni, A. Dandekar, D.K. Das, Experimental investigation of viscosity and specific heat of silicon dioxide nanofluids, Micro & Nano Letters 2 (2007) 67–71.
[32] F.C. McQuiston, J.D. Parker, J.D. Spitler, Heating Ventilating and Air Conditioning, 6th ed, John Wiely & Sons, Inc, New York, 2005.
[33] S.Y. Chen, C.Y. Tang, W.T. Chuang, J.J. Lee, Y.L. Tasi, J.C.C. Chan, C.Y. Lin, Y.C. Liu, S. Cheng, A facile route to synthesizing functionalized mesoporous SBA-15 materials with platelet morphology and short mesochannels, Chemistry of Materials 20 (2008) 3906–3916.
[34] N.A. Stephenson, A.T. Bell, The influence of substrate composition on the kinetics of olefin epoxidation by hydrogen peroxide catalyzed by iron (III) [tetrakis (pentafluorophenyl)] porphyrin, Journal of Molecular Catalysis A 285 (2006) 231–235.
[35] P. Innocenzi, P. Falcaro, D. Grosso, F. Babonneau, Order–disorder transitions and evolution of silica structure in self-assembled mesostructured silica films studied through FTIR spectroscopy, Journal of Physical Chemistry B 107 (2003) 4711–4717.
[36] D.Y. Zhao, Q.S. Huo, J.L. Feng, B.F. Chmelka, G.D. Stucky, Nonionic triblock and star diblock copolymer and oligomeric surfactant syntheses of highly ordered, hydrothermally stable, mesoporous silica structures, Journal of the American Chemical Society 120 (1998) 6024–6036.
[37] ASHRAE Handbook, American Society of Heating, Refrigerating and Air-conditioning Engineers, Fundamentals, Atlanta, GA, 1997.
[38] S. Thomas, C.B. Sobhan, A review of experimental investigations on thermal phenomena in nanofluids, Nanoscale Research Letters 6 (2011) 377–397.
[39] L.S. Sundar, E.V. Ramana, M.K. Singh, A.C.M. Sousa, Viscosity of low volume concentrations of magnetic Fe3O4 nanoparticles dispersed in ethylene glycol and water mixture, Chemical Physics Letters 554 (2012) 236–242.
[40] V. Kunaresan, R. Velraj, Experimental investigation of the thermophysical properties of water–ethylene glycol mixture based CNT nanofluids, Thermochimica Acta 545 (2012) 180–186.
[41] H.Q. Xie, J.C. Wang, T.G. Xi, Y. Liu, F. Ai, Dependence of the thermal conductivity of nanoparticles–fluid mixture on the base fluid, Journal of Materials Science Letters 21 (2002) 1469–1471.
[42] T.T. Baby, R. Sundara, Synthesis and transport properties of metal oxide decorated grapheme dispersed nanofluids, Journal of Physical Chemistry C 115 (2011) 8527–8533.
[43] N. Shalkevich, A. Shalkevich, T. BÜrgi, Thermal conductivity of concentrated colloids in different states, Journal of Physical Chemistry C 114 (2010) 9568–9572.
[44] P. Warrier, Y. Yaun, M.P. Beck, A.S. Teja, Heat transfer in nanoparticles suspensions: modeling the thermal conductivity of nanofluids, AIChE Journal 56 (2010) 3243–3256.
[45] H.E. Patel, S.K. Das, T. Sundararajan, A.S. Nair, B. George, T. Pradeep, Thermal conductivity of naked and monolayer protected metal nanoparticles based nanofluids: manifestation of anomalous enhancement and chemical effects, Applied Physics Letters 83 (2003) 2931–2933.
[46] E.V. Timofeeva, W. Yu, D.M. France, D. Singh, J.L. Routbort, Base fluid and temperature effects on the heat transfer characteristics of SiC in ethylene glycol/H_2O and H_2O fluid, Journal of Applied Physics 109 (2011) 14914–14918.
[47] D.H. Yoo, K.S. Hong, H.S. Yang, Study of thermal conductivity of nanofluids for application of heat transfer fluids, Thermochimica Acta 455 (2007) 66–69.